



---

# Audio Engineering Society

# Convention Paper 6780

Presented at the 120th Convention  
2006 May 20–23 Paris, France

*This convention paper has been reproduced from the author's advance manuscript, without editing, corrections, or consideration by the Review Board. The AES takes no responsibility for the contents. Additional papers may be obtained by sending request and remittance to Audio Engineering Society, 60 East 42<sup>nd</sup> Street, New York, New York 10165-2520, USA; also see [www.aes.org](http://www.aes.org). All rights reserved. Reproduction of this paper, or any portion thereof, is not permitted without direct permission from the Journal of the Audio Engineering Society.*

---

## Efficient resonant loudspeakers with large form-factor design freedom

Ronald M. Aarts<sup>1</sup>, Joris A.M. Nieuwendijk<sup>1</sup>, and Okke Ouweltjes<sup>1</sup>

<sup>1</sup>*Philips Research, High Tech Campus 36, NL-5656 AE Eindhoven, The Netherlands*

Correspondence should be addressed to Ronald M. Aarts ([Ronald.M.Aarts@Philips.com](mailto:Ronald.M.Aarts@Philips.com))

### ABSTRACT

Small cabinet loudspeakers with a flat response are quite inefficient. Assuming that the frequency response can be manipulated electronically, systems that have a non-flat SPL-response can provide greater usable efficiency. Such a non-flat design can deal with very compact housing, but, for small drivers, it would require a relatively large cone excursion to obtain a high SPL. However, mounting the driver in a pipe, the air column can be made to resonate which enables the use of small drivers with a small cone excursion to obtain a high SPL. For these special loudspeakers, a practically relevant optimality criterion, involving the driver- and pipe parameters, will be defined. This can be especially valuable in designing very compact loudspeaker systems. An experimental example of such a design is described and a working prototype is presented.

### 1. INTRODUCTION

There is a longstanding interest in obtaining a high sound output from compact loudspeaker arrangements. The introduction of concepts such as Flat TV and 5.1 channel sound reproduction systems has led to a renewed interest in obtaining a high sound output from compact loudspeaker arrangements with a high efficiency. Compact relates here to both the volume of the cabinet into which the loudspeaker is mounted as well as the cone area of the loudspeaker. In conventional loudspeaker system design, the force factor  $Bl$  is chosen in relation to enclosure volume, suspension stiffness, cone diam-

eter, and moving mass to yield a flat response over a specified frequency range. For small cabinet loudspeakers such a design is in general quite inefficient. It is not possible to combine a very high efficiency and a high sensitivity in a wide frequency range with a compact arrangement. On the other hand, assuming that the frequency response can be manipulated electronically, it then turns out that systems having a non-flat sound-pressure level (SPL) can provide greater usable efficiency, at least over a limited frequency range [1, 2, 3]. Such a design can deal with very compact housing, but requires for small drivers a large cone displacement to obtain a high

SPL. However, using a pipe, the air column in the pipe can be made in resonance which enables the use of small drivers to obtain a high SPL.

In the past much effort has been spent regarding higher order band-pass systems using pipes, see e.g. [4, 5, 6]. However, focus in that work was on designing systems with a reasonably broad bandwidth, while we are aiming for the highest efficiency which implies a very small bandwidth, and hence a high quality factor. We discuss these special resonant loudspeakers which have a high SPL but require only a very low cone displacement. The dependence on the behavior of the transducer and its housing on various parameters, in particular the force factor  $Bl$  and pipe dimensions, is investigated. For these special loudspeakers, a practically relevant optimality criterion, involving the loudspeaker and pipe parameters, will be defined. The desired characteristics are obtained at the expense of a decreased sound quality and the requirement of some additional electronics. It is discussed how such a special loudspeaker can be made. It appears to be very cost-efficient and low-weight, and has a high degree in form factor freedom of its cabinet. An example of such a design is described and the performance of a working prototype is presented.

## 2. SPECIAL RESONANT LOUDSPEAKERS WITH A HIGH QUALITY FACTOR $Q$

There are well-known loudspeaker systems indicated as ‘Acoustic Labyrinth Loudspeaker’ from [7], see Figs. 1 and 2. In such constructions, the driver is mounted into a relatively long duct with a length approximately equal to one quarter of the wave length corresponding to the open air resonance frequency of the driver. However, those systems did not aim for a high quality factor  $Q$ . Olney wanted to lower the  $Q$ , from curve A into curve B of the SPL response of right panel of Fig. 2.

The essential feature of the present work is that we are aiming for a high  $Q$  of the system by using a system with a relatively long pipe as shown schematically in Fig. 3. A specified frequency  $f_{work}$  substantially coincides with the Helmholtz frequency, or anti-resonance frequency as shown as  $f_b$  in Fig. 4. This  $f_{work}$  is the frequency (or a very narrow band) to which the low frequency content of the signal is transferred, conforming to the mapping principle as



FIG. 1. Acoustical labyrinth with back removed.

Fig. 1: Olney’s ‘Acoustic Labyrinth Loudspeaker’ [7].

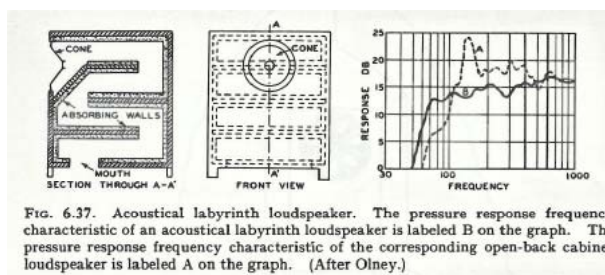


FIG. 6.37. Acoustical labyrinth loudspeaker. The pressure response frequency characteristic of an acoustical labyrinth loudspeaker is labeled B on the graph. The pressure response frequency characteristic of the corresponding open-back cabinet loudspeaker is labeled A on the graph. (After Olney.)

Fig. 2: ‘Acoustic Labyrinth Loudspeaker’ from Olson [8]. Olney’s aim was to lower the high  $Q$  curve A into curve B of the SPL-response.

introduced in [2], and which is further discussed in Sec. 3. The Helmholtz frequency  $f_b$  is the frequency where the electric input impedance curve reaches a local minimum between the first two impedance peaks, see Fig. 4. This is in contrast to [9]. There

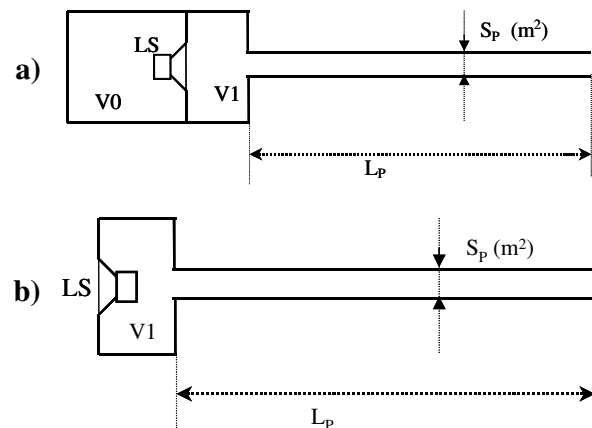


Fig. 3: Schematic construction of the loudspeaker. a) Upper panel: band-pass enclosure with long port. b) Lower panel: bass-reflex enclosure with long port.

we used the fundamental resonance frequency of the system determined by the closed volume of the enclosure and the driver, while the modes of the enclosure were outside the frequency region of interest. With a band-pass box, the working frequency  $f_{work}$  then coincides preferably with  $f_1$ , the first resonance frequency of the system, see Fig. 4, whereas in the reflex box case, the second resonance frequency is utilized ( $f_2$  in Fig. 4). We define a frequency  $f_0$  in the case of Fig. 3-a as the resonance frequency of the box with closed volume  $V_0$  plus the driver, in absence of volume  $V_1$  and pipe. In the case of Fig. 3-b  $f_0 = f_s$ , where  $f_s$  is, as usual, the free air resonance frequency of the driver. With a band-pass box design, usually  $f_0$  coincides with  $f_b$ . However, in our application  $f_0$  can differ considerably from  $f_b$ . To be more precise we allow values of  $f_0$  within the range

$$0.4f_b < f_0 < 2.5f_b. \quad (1)$$

In Fig. 5 the impedances and velocities occurring in the system's pipe of cross-sectional area  $S_p$  and length  $L_p$  are given. The band-pass system is mod-

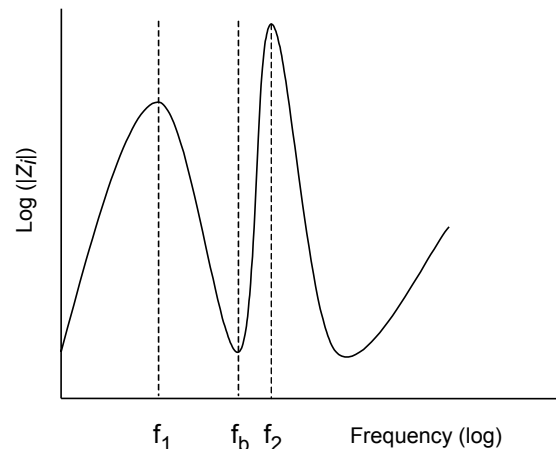


Fig. 4: The impedance of the driver mounted in a pipe. The relevant frequencies are the resonance frequencies  $f_1$  and  $f_2$ , and the Helmholtz frequency or anti-resonance frequency  $f_b$ .

eled with the lumped element model according to Fig. 6. The elements shown in Fig. 6 are given in Table 1. Further we have for the total spring constant of the driver suspension and the back volume  $V_0$  (if there is any)

$$k^* = C_{ms}^{-1} + \frac{\rho_0 c_0^2 S_1^2}{V_0}, \quad (2)$$

where  $\rho_0$  is the density, and  $c_0$  the speed of sound of the medium, and  $C_1 = V_1/(\rho_0 c_0^2 S_1^2)$  is the mechanical compliance of the front volume  $V_1$ .

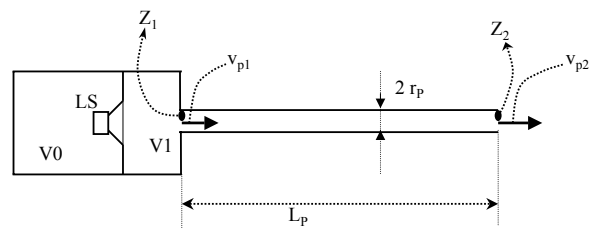


Fig. 5: The mechanical impedances  $Z_1$  and  $Z_2$ , and velocities  $v_{p1}$  and  $v_{p2}$  in the system's pipe.

If the air is harmonically vibrating with a frequency corresponding with the wavenumber  $k = \omega/c$  and

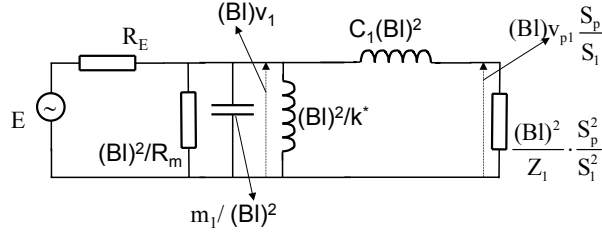


Fig. 6: The mobility-type lumped-element model of the system according to Fig. 5,  $v_1$  is the cone velocity, other parameters are in Table 1.

velocity  $v_{p1}$ , then the input mechanical impedance  $Z_1$  is given by [9]

$$Z_1 = \rho_0 c_0 S_p \frac{\frac{Z_2}{\rho_0 c_0 S_p} \cos kL_p + j \sin kL_p}{j \frac{Z_2}{\rho_0 c_0 S_p} \sin kL_p + \cos kL_p}. \quad (3)$$

The velocity at the end of the pipe is

$$v_{p2} = \frac{v_{p1}}{j \frac{Z_2}{\rho_0 c_0 S_p} \sin kL_p + \cos kL_p}. \quad (4)$$

Looking at Eq. 4, we see that at frequencies such that  $Z_2 \ll \rho_0 c_0 S_p$  and  $\sin kL_p \approx 1$ , that  $v_{p2}$  can be much larger than  $v_{p1}$ . For these frequencies we get a gain of

$$\frac{v_{p2}}{v_{p1}} \approx \frac{\rho_0 c_0 S_p}{j Z_2}. \quad (5)$$

It is this gain that we want to exploit. Usually, in higher order band-pass systems, one wants a certain bandwidth but because we are interested to make a resonator, the bandwidth may be very small. The only limitation is the quality factor  $Q_p$  of the pipe, which is discussed in Appendix A. In order to optimize the SPL for a certain but fixed input power, we need to exploit the port resonance and to optimize the force factor  $Bl$  for a given system geometry. This particular optimal value for the force factor we denote as  $Bl_o$ .

In the following we want to calculate the SPL of the system. Therefore we need first to calculate the acoustic power  $P_a$  delivered by the system. Using Eq. 3 to determine  $Z_1$  from  $Z_2$ , Fig. 6 to determine the cone velocity  $v_1$ , and  $v_{p1}$ , and Eq. 4 to determine  $v_{p2}$  from  $v_{p1}$ , we can calculate the radiated acoustic

power  $P_a$  at the opening of the pipe as

$$P_a = \frac{1}{2} |v_{p2} S_p|^2 R_{arad}, \quad (6)$$

where

$$R_{arad} = \frac{\rho_0 \omega^2}{2\pi c_0}, \quad (7)$$

is the approximated real part of the radiation impedance  $Z_2$  in the low frequency  $2\pi$  field. The relation between SPL at 1 m distance and  $\eta$  [2, Eq. 32] is

$$\text{SPL} = 112.18 + 10 \log \eta, \quad (8)$$

where the system's efficiency is

$$\eta(\omega) = P_a / P_e \quad (9)$$

and  $P_e$  is the electrical power fed to the system, which we consider in the following equal to 1 W (@ 2.8  $\Omega$  and 1.67 V<sub>RMS</sub>). Using Eqs. 6 and 8 we get the desired value for the SPL. The aim is to get the highest possible SPL, but this results in a narrow peak around  $f_{work}$ , with a high  $Q$ . It appears—like for the closed box system [2]—that if  $Bl$  is approximately equal to the optimal  $Bl$  that the highest peak in the SPL curve is reached and that we have for the electrical input impedance

$$|Z_i|_{f=f_b} \approx 2R_E. \quad (10)$$

This relation appears to be very practical to see whether the optimal  $Bl_o$  has been chosen.

## 2.1. Resonant band-pass loudspeaker

Figure 7 displays the SPL in dB as a function of frequency (solid-thick-blue curve), for the system shown in Fig. 3-a; where  $m_1$  has been increased to 24 g in order to obtain  $f_0 = f_b = 55$  Hz,  $Bl$  has the theoretical optimal value of  $Bl_o = 11.7$ , and  $V_0 = 2.1$ . As a comparison the dashed red curve shows the SPL of the same driver mounted in an infinite baffle with the same excursion as in the band-pass box. Figure 7 clearly shows the extra gain in SPL we get as the difference between the peak and dip of both curves at 55 Hz, which is a result of Eq. 5. Figure 8 shows the corresponding electrical impedance of the system.

The local minimum between the first peaks in Fig. 8 equals 5.6  $\Omega$ , this conforms to Eq. 10,  $2R_{DC}$ . In Fig. 9, the actual loudspeaker cone displacement is given. The maximum displacement reduction of the

Table 1: Fitted parameters of the prototype's loudspeaker and pipe.

|                               |           |         |                   |
|-------------------------------|-----------|---------|-------------------|
| free air resonance frequency  | $f_s$     | 83.79   | (Hz)              |
| mechanical quality factor     | $Q_{ms}$  | 4.14    | (-)               |
| electrical quality factor     | $Q_{es}$  | 0.429   | (-)               |
| total quality factor          | $Q_{ts}$  | 0.389   | (-)               |
| equivalent acoustic volume    | $V_{as}$  | 0.365   | (l)               |
| voice coil DC Resistance      | $R_E$     | 2.80    | ( $\Omega$ )      |
| total moving mass             | $m_1$     | 0.0088  | (kg)              |
| mechanical compliance         | $C_{ms}$  | 0.00041 | (m/N)             |
| mechanical resistance         | $R_m$     | 1.12    | (Ns/m)            |
| motor force factor            | $Bl$      | 5.50    | (N/A)             |
| membrane area                 | $S_1$     | 0.0025  | (m <sup>2</sup> ) |
| reference efficiency          | $\eta$    | 0.00049 | (%)               |
| produced sound pressure level | SPL       | 79.076  | (dB)              |
| series lossless inductance    | $L_1$     | 0.00044 | (H)               |
| mass                          | $C_{mes}$ | 0.00029 | (F)               |
| compliance                    | $L_{ces}$ | 0.0124  | (H)               |
| mechanical losses             | $R_{es}$  | 27.009  | ( $\Omega$ )      |
| Helmholtz frequency           | $f_b$     | 55      | (Hz)              |
| front volume                  | $V_1$     | 0.9     | (l)               |
| port length                   | $L_p$     | 1.00    | (m)               |
| Eff. port length              | $L'_p$    | 1.03    | (m)               |
| port area                     | $S_p$     | 0.00145 | (m <sup>2</sup> ) |
| port losses                   | $R_p$     | 0.01575 | (Ns/m)            |
| port losses                   | $Q_p$     | 30      | (-)               |

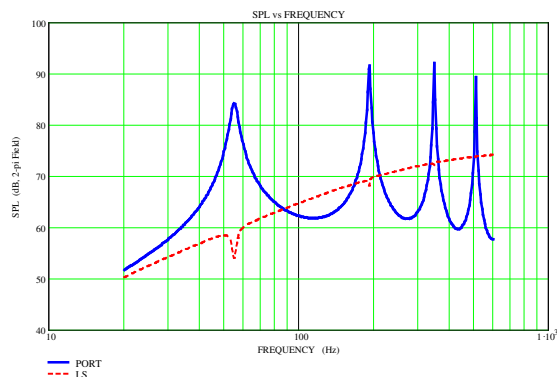


Fig. 7: SPL as a function of frequency. Port-only: solid-thick-blue curve. Same loudspeaker in an infinite baffle with the same excursion as the band-pass box: dashed red curve. The parameters are according to Table 1, except for  $m_1$  which has been increased to 24 g in order to obtain  $f_0 = f_b = 55$  Hz,  $Bl$  has the theoretical optimal value of  $Bl_o = 11.7$ , and  $V_0 = 2$  l.

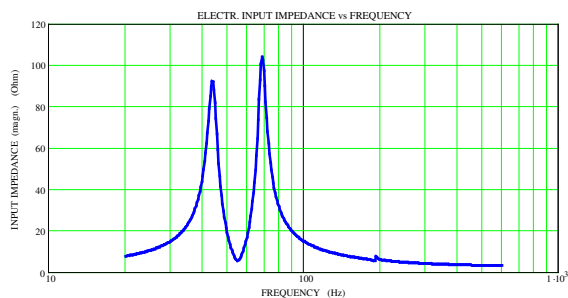


Fig. 8: Electric input impedance (magnitude) as a function of frequency. The parameters are according to Table 1, except for  $m_1$  which has been increased to 24 g in order to obtain  $f_0 = f_b = 55$  Hz,  $Bl$  has the theoretical optimal value of  $Bl_o = 11.7$ , and  $V_0 = 2$  l.

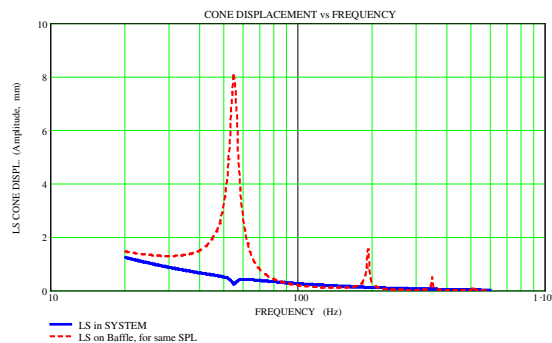


Fig. 9: Cone displacement as a function of frequency. Loudspeaker in system: solid-thick-blue curve. Same loudspeaker in an infinite baffle with the same SPL as the band-pass box: dashed red curve. The parameters are according to Table 1, except for  $m_1$  which has been increased to 24 g in order to obtain  $f_0 = f_b = 55$  Hz,  $Bl$  has the theoretical optimal value of  $Bl_o = 11.7$ , and  $V_0 = 2$  l.

driver, see Fig. 9, coincides exactly with the position of the top of the SPL-curve of Fig. 7.

## 2.2. Resonant reflex loudspeaker

Similar to the previous section, we will now study the reflex system of Fig. 3-b. In Fig. 10, the SPL of a system according to Fig. 3-b is shown. We see that around the work frequency  $f_{work} = f_b$ , the SPL of the reflex- and band-pass system are practically the same due to the very low displacement of the loudspeaker. A deviation from the optimum value of  $Bl$  is not critical, provided that it is not too large. In Fig. 11 an example of a non-optimal  $Bl$ -value is given. In this case, with the same configuration as in Fig. 10,  $Bl$  has the value 2, i.e. a factor 0.17 of the optimal  $Bl$ -value. It appears that the maximum output no longer coincides with  $f_{work}$  of 55 Hz. The cone displacement reduction is much less substantial and not coinciding with the frequency giving maximum SPL, also—but not shown here—the input impedance  $Z_i \neq 2R_E$ . In Fig. 12 an example is given of the case that  $f_b \neq f_0 = 84$  Hz, with a driver having—according to Table 1— $Bl = 5.5$ .

Fig. 13 shows the corresponding electric input impedance curve. Figure 12 shows—despite  $f_b \neq f_0$ —that the SPL curve resembles the one of Fig. 10.

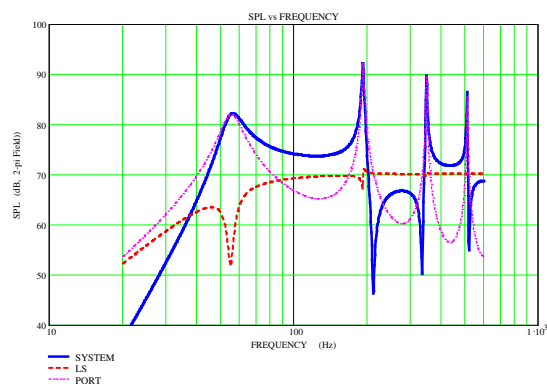


Fig. 10: SPL as a function of frequency for the bass reflex enclosure as Fig. 3-b. System: solid-thick-blue curve. Loudspeaker: medium-thick dashed red curve. Port only: thin-dashed magenta curve. The parameters are according to Table 1, except  $m_1 = 20.4$  g in order to obtain  $f_0 = f_b = 55$  Hz.

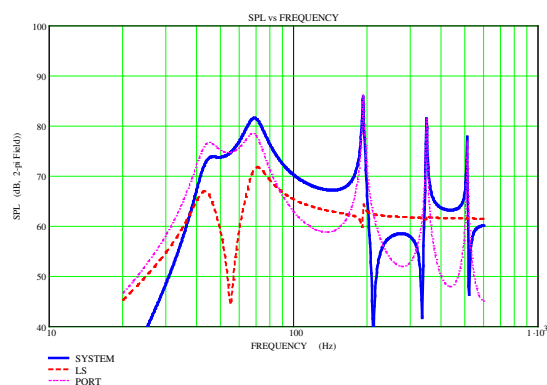


Fig. 11: SPL as a function of frequency for the bass reflex enclosure of Fig. 3-b with a non-optimal  $Bl$ -value. System: solid-thick-blue curve. Same loudspeaker: medium-thick dashed red curve. Port only: thin-dashed magenta curve. The parameters are according to Table 1, except  $m_1 = 20.4$  g and  $Bl = 2$ , which is a factor 0.17 smaller than the optimal value  $Bl_o = 11.7$ .

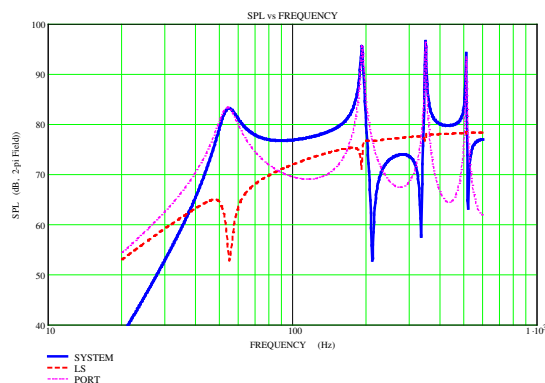


Fig. 12: SPL as a function of frequency for the bass reflex enclosure of Fig. 3-b, where  $f_0 \neq f_b$ ,  $f_0 = f_s = 84$  Hz. System: solid-thick-blue curve. Same loudspeaker: medium-thick dashed red curve. Port only: thin-dashed magenta curve. The parameters are according to Table 1.

The fact that  $f_b$  and  $f_0$  do not necessarily need to be equal, gives more design freedom. A practical consequence, for example, is that if  $f_0 > f_b$  then the moving mass does need not to be increased to lower  $f_0$ .

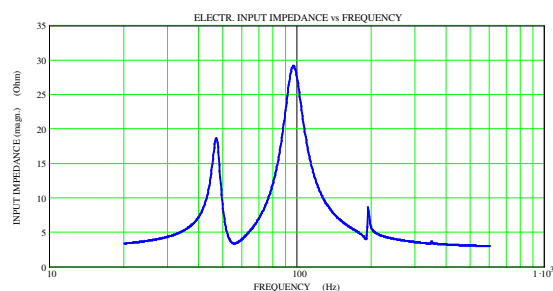


Fig. 13: Electric input impedance (magnitude) as a function of frequency corresponding to Fig. 12, where  $f_0 \neq f_b$ ,  $f_0 = f_s = 84$  Hz.

To demonstrate the large form-factor design freedom, one of the prototypes is shown in two different viewpoints in Fig. 14, which is a folded version of Fig. 3-b. The loudspeakers are mounted on top. We used two because a single one with the desired cone area and  $Bl$  was not available.



Fig. 14: Drawing of the the experimental set-up. The opening at the front of the pipe in the left drawing is the ‘end of the pipe’. The cavity between the drivers and the grey upper disc is volume  $V_1$ .

### 3. FREQUENCY MAPPING

Due to the typical high and narrow peak in the frequency response, see Fig. 7, the normal operating range of the driver decreases considerably. This makes the driver unsuitable for normal use. To overcome this, a second measure is applied. Non-linear processing essentially compresses the bandwidth of a 20 to 120 Hz 2.5-octave bass signal down to a much narrower span, which is centered at the SPL peak of the system. This can be done with a set-up as depicted in Fig. 15 and will be discussed below.

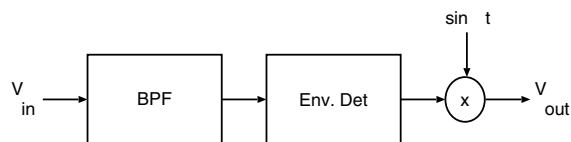


Fig. 15: Set-up of the mapping scheme. The boxes labeled ‘BPF’ and ‘Env. Det.’ are a band-pass filter and envelope detector, respectively. The sinusoid has a fixed frequency equal to  $f_{work}$ . The signal  $V_{out}$  is fed to the power amplifier and finally to the driver.

The band-pass filter takes the band of interest, typically 20–120 Hz, and the envelope detector deter-

mines the envelope  $m(t)$  of this signal. Then  $m(t)$  is multiplied with a sinusoid of fixed amplitude and fixed frequency  $f_{work}$ . The result is that the coarse structure  $m(t)$  (the envelope) of the music signal after the compression or ‘mapping’ is the same as before the mapping. Only the fine structure has been changed to a sinusoid of fixed frequency  $f_{work}$  which coincides with the peak in the SPL response.

### 4. EXPERIMENTAL RESULTS

The frequency response and the electric input impedance of the system, as shown in Fig. 3-b. was measured. The measured impedance was used to determine the driver and pipe parameters which are listed in Table 1. The open end of the pipe, the other side, and the microphone were at the corners of an equilateral triangle with sides of 1 m. The frequency response of the system when driven with 1 W power is shown in Fig. 16 (solid-blue curve). The frequency response was computed as well. The pipe length  $L_p$  and the  $Q_p$  of the model parameters were chosen such that it resembles the measurement. The computed result is plotted as the dashed-red curve in Fig. 16. The corresponding measured and calculated electric impedance of the system is shown in Fig. 17. It appears that the computed result matches the measured result quite well, this is while the parameters  $L_p$  and  $Q_p$  are sensibly chosen as discussed below. The physical length  $L_p$  of the pipe is equal to 1 m. Due to the complex radiation impedance of the pipe, it seems that the pipe is longer. This is known as the end correction [9]

$$L'_p = L_p + 0.6r_p. \quad (11)$$

When the port losses  $R_p = 0.01575$  Ns/m are introduced into the calculation we get a good resemblance with the measured data. We consider  $R_p$  here as a total (including the radiation losses) lumped mechanical-impedance parameter at the end of the port, i.e.  $R_p$  is equal to the real part of  $Z_2$  (see Fig. 5), while for the radiation computations we use Eqs. 6–7. To demonstrate this effect: if we neglect the port losses we obtain the curves corresponding to Figs. 16 and 17 shown in Figs. 18 and 19 respectively, which shows that the peak in the SPL around 55 Hz could have been a little higher. It appears also that the other peaks at higher frequencies become much higher.

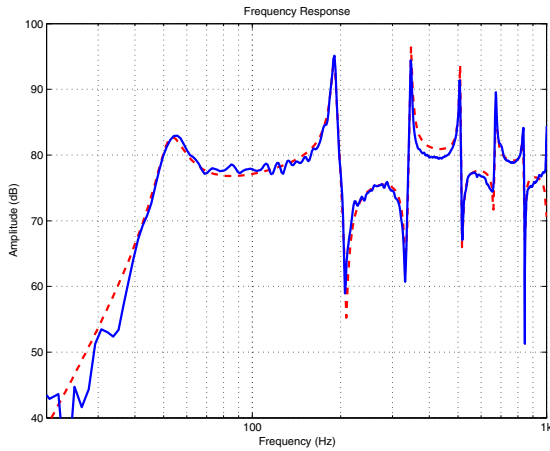


Fig. 16: Measured and calculated frequency response of the system as shown in Figs. 3-b. The port damping in the calculation was  $R_p = 0.01575$  Ns/m. Solid-blue curve: measurement, dashed-red curve: calculation.

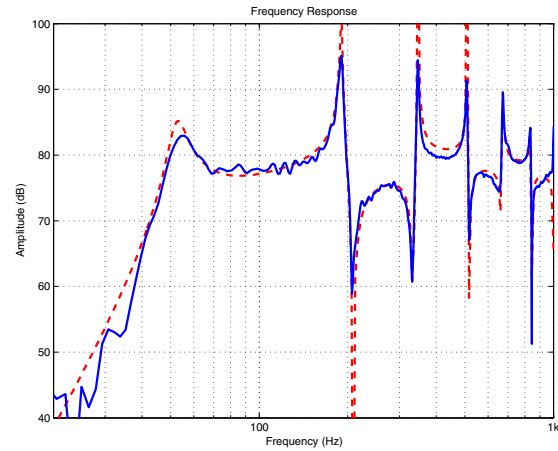


Fig. 18: Measured and calculated frequency response of the system as shown in Figs. 3-b. The port damping was almost neglected in the calculation. Solid-blue curve: measurement, dashed-red curve: calculation.

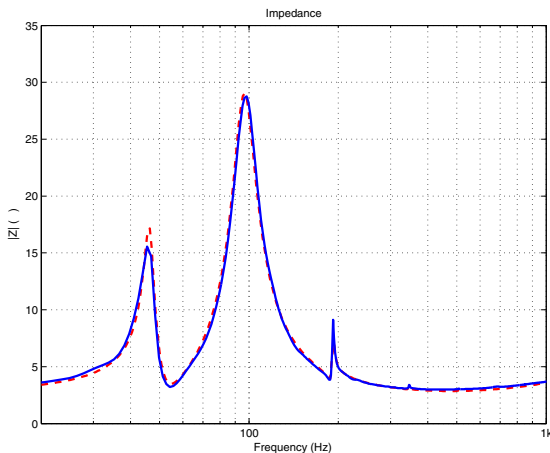


Fig. 17: Measured and calculated electric impedance of the system as shown in Figs. 3-b. The port damping in the calculation was  $R_p = 0.01575$  Ns/m. Solid-blue curve: measurement, dashed-red curve: calculation.

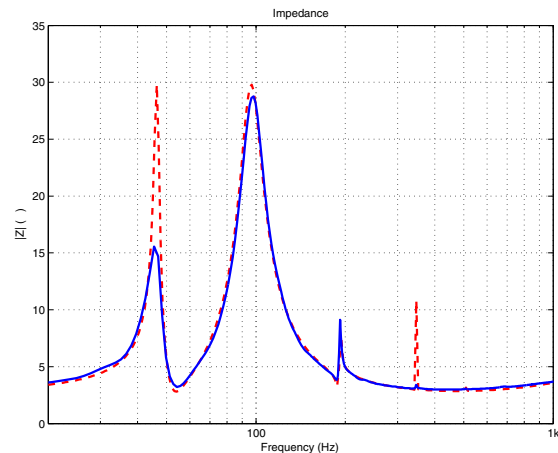


Fig. 19: Measured and calculated electric impedance of the system as shown in Fig. 3-b. The port damping was almost neglected in the calculation. Solid-blue curve: measurement, dashed-red curve: calculation.

## 5. DISCUSSION

An old loudspeaker designer's dilemma is 'do we want a high efficiency or small enclosure?'. This dilemma is partially solved by using the high-Q band-pass box concept as discussed above, however, at the expense of a decreased sound quality and the need for some additional electronics to accomplish the frequency mapping. While the new driver is not a HiFi one, many informal listening tests and demonstrations<sup>1</sup> confirmed that the decrease of sound quality appears to be modest; apparently because the auditory system is less sensitive at low frequencies. Also, the other parts of the audio spectrum have a distracting influence on this mapping effect, which has been confirmed during formal listening tests [10], where the detectability of mis-tuned fundamental frequencies was determined for a variety of realistic complex signals. Finally, the part of the spectrum which is affected is only between say 20 to 120 Hz, so the higher harmonics of these low notes are mostly out of this band and are thus not affected. They will contribute in their normal un-processed fashion to the missing fundamental effect. All these factors support the notion that detuning becomes difficult to detect once the target complex is embedded in a spectrally and temporally *rich* sound context, as is typical for applications in modern multimedia reproduction devices [10].

## 6. CONCLUSIONS

The force factor  $Bl$ , enclosure, and port design play a very important role in loudspeaker design. It determines the efficiency, the sensitivity, the impedance, the SPL response, the weight, and the cost. It appears to be not possible to obtain both a high efficiency as well as a high sensitivity in a wide frequency range. A new loudspeaker has been developed, which, together with some additional electronics, yields a large form-factor design freedom. Additionally, it can be a low-cost, lightweight, compact, sensitive, and efficient loudspeaker system which is very suitable for low-frequency sound reproduction.

<sup>1</sup>Demonstrations are on <http://www.dse.nl/~rmaarts>

## 7. REFERENCES

- [1] E. Larsen and R.M. Aarts. *Audio Bandwidth extension. Application of Psychoacoustics, Signal Processing and Loudspeaker Design*. J. Wiley, September 2004. ISBN 0470 85864 8.
- [2] R.M. Aarts. High-Efficiency Low-BI Loudspeakers. *J. Audio Eng. Soc.*, 53(7):579–592, July/August 2005.
- [3] R.M. Aarts. Optimally sensitive and efficient compact loudspeakers. *J. Acoust. Soc. Am.*, 119(2):890–896, February 2006.
- [4] L.R. Fincham. A bandpass loudspeaker enclosure. *Preprint 1512 63rd AES Convention, April, 1979*.
- [5] E.R. Geddes. An introduction to band-pass loudspeaker systems. *J. Audio Eng. Soc.*, 37(5):308–342, May 1989.
- [6] J.A.M. Nieuwendijk. Band-pass loudspeaker enclosure with a long port. *Preprint 3508 94th AES Convention Berlin, 1993 March 16–19, 1993*.
- [7] B. Olney. A method of eliminating cavity resonance, extending low frequency response and increasing acoustic damping in cabinet type loudspeakers. *J. Acoust. Soc. Am.*, 8(2):104–111, 1936.
- [8] H.F. Olson. *Acoustical engineering*. Van Nostrand, 1957.
- [9] L.E. Kinsler, A.R. Frey, A.B. Coppens, and J.V. Sanders. *Fundamentals of acoustics*. J. Wiley, 1982.
- [10] Nicolas Le Goff, R.M. Aarts, and A.G. Kohlrausch. Thresholds for hearing mistuning of the fundamental component in a complex sound. In *Proceedings of the 18th International Congress on Acoustics (ICA2004), Paper Mo.P3.21, p. I-865, (Kyoto, Japan), 2004*.
- [11] M.J. Moloney and D.L. Hatten. Acoustic quality factor and energy losses in cylindrical pipes. *American Journal of Physics*, 69(3):311–314, March 2001.

## APPENDIX A: THE ACOUSTIC QUALITY FACTOR OF THE PORT

The quality factor  $Q_p$  is defined [11] as

$$Q_p = \frac{\omega E_{tot}}{P_{tot}}, \quad (12)$$

where  $P_{tot}$  is the total port power due to radiation, thermal and viscous losses, and is related to the total (lumped) port losses  $R_p$  as

$$P_{tot} = \frac{1}{2}|v_{p2}|^2 R_p. \quad (13)$$

In simple harmonic motion, the total energy in a cylindrical pipe containing a standing sinusoidal wave with maximal velocity  $v_{p2}$  at one end may be written as the maximum kinetic energy which is equal to

$$E_{tot} = \frac{1}{4}\rho v_{p2}^2 S_p L_p. \quad (14)$$

Combining Eqs. 12–14 results in

$$Q_p = \frac{\omega \rho S_p L_p}{2R_p}, \quad (15)$$

or for a pipe of length  $L_p = \lambda/4 = \frac{c}{4f}$

$$Q_p = \frac{\pi S_p \rho c}{4R_p}. \quad (16)$$

This Eq. 16 is a convenient way to relate the total pipe losses  $R_p$  to the total  $Q_p$  of a quarter-lambda pipe. The  $Q$  due to the radiation ( $2\pi$ -field) only is

$$Q_{rad} = \frac{cL_p}{2S_p f}, \quad (17)$$

and for a baffled quarter-lambda pipe

$$Q_{rad} = \frac{c^2}{8S_p f^2}. \quad (18)$$

For frequencies in the bass range we get—using Eq. 18—values for  $Q_{rad}$  which are more than ten times higher than the observed total  $Q_p$  which is usually less than 50. Apparently, the radiated acoustic power contributes only in a very small extent to the total damping ( $R_{rad} \ll R_p$ ).